

BELLCOMM, INC.

1100 SEVENTEENTH STREET, N.W. WASHINGTON, D.C. 20036

COVER SHEET FOR TECHNICAL MEMORANDUM

TITLE- Unmanned Entry into the Venusian
Atmosphere

TM- 67-1013-6

DATE- July 24, 1967

FILING CASE NO(S)- 233

AUTHOR(S)- D. E. Cassidy

FILING SUBJECT(S)- Venus
(ASSIGNED BY AUTHOR(S)- Entry Trajectories

ABSTRACT

The high density structure of the Venusian atmosphere as presently conceived almost certainly guarantees successful entry in terms of energy dissipation. The high entry velocities ranging from 40,000 fps to over 50,000 fps associated with several manned flyby trajectories, however, dictate the use of shallow entry corridors resulting in restrictive operational capability. Small, low ballistic parameter atmospheric probes will not be as restricted as larger payload probes.

Following entry and deceleration, low rates of sink are achieved at high altitudes resulting in large dispersions in time to fall due to uncertainties in the atmospheric density. The low rates of sink, though, permit high altitude deployment of payloads.

In spite of the high temperatures in lower atmosphere, it is quite feasible to "target" for a temperate region which occupies an altitude band between 125,000 ft. and 215,000 ft.

Following entry, a typical entry probe will be in line of sight to the manned flyby spacecraft for a 1.5 to 2 hour period during spacecraft periapsis passage. Longer communications periods will require an orbiter data link.

(NASA-CR-88181) UNMANNED ENTRY INTO THE
VENUSIAN ATMOSPHERE (Bellcomm, Inc.) 32 P

N79-73430

Unclas
00/91 12928
(CODE)

FACILITY

(PAGES)

(NASA CR OR TM OR RS NUMBER)

(CATEGORY)

30

SEE REVERSE SIDE FOR DISTRIBUTION LIST

DISTRIBUTION

COMPLETE MEMORANDUM TO

CORRESPONDENCE FILES:

OFFICIAL FILE COPY
plus one white copy for each
additional case referenced

TECHNICAL LIBRARY (4)

NASA Headquarters

Messrs. P. E. Culbertson/MLA
J. H. Disher/MLD
F. P. Dixon/MTY
E. W. Hall/MTS
T. A. Keegan/MA-2
D. R. Lord/MTD
M. J. Raffensperger/MTE
L. Reiffel/MA-6
A. D. Schnyer/MTV
G. S. Trimble/MT

MSC

Messrs. M. A. Silveira/ET-25
W. E. Stoney, Jr/ET
J. M. West/AD

MSFC

Messrs. R. J. Harris/R-AS-VP
B. G. Noblitt/R-AERO-DPF
F. L. Williams/R-AS-DIR

KSC

Messrs. J. P. Claybourne/EDV-4
R. C. Hock/PPR-2
N. P. Salvail/MC

AMES RESEARCH CENTER

Mr. L. Roberts/M

Bellcomm

Messrs. F. G. Allen
G. M. Anderson
A. P. Boysen
J. P. Downs

Bellcomm (Cont'd)

Messrs. D. R. Hagner
P. L. Havenstein
J. J. Hibbert
W. C. Hittinger
B. T. Howard
D. B. James
H. S. London
K. E. Martersteck
R. K. McFarland
J. Z. Menard
I. D. Nehama
G. T. Orrok
I. M. Ross
R. L. Selden
R. V. Sperry
J. M. Tschirgi
R. L. Wagner
J. E. Waldo
All Members, Division 101
Department 1023

SUBJECT: Unmanned Entry into the
Venusian Atmosphere
Case 233

DATE: July 24, 1967

FROM: D. E. Cassidy

TM-67-1013-6

TECHNICAL MEMORANDUM


INTRODUCTION

For manned planetary flyby missions during the various Mars and Venus opportunities in the late 1970's, considerable attention will be given to experiments performed during the planetary encounter periods. A number of these experiments will be performed close to or on the planet surface, requiring penetration into the planetary atmospheres. The constraints imposed by atmospheric entry on the overall mission in terms of entry probe weights and sizes and operational requirements are then of considerable interest to mission planning. The purpose of this memo is to address these questions associated with the Venus encounters and to develop a basic strategy for defining complements of entry probes.

ENTRY CONDITIONS

The typical missions considered in this analysis are the 1975 single-planet, 1977 triple-planet, and the 1976 and 1978 dual-planet flybys. The entry velocities associated with these opportunities are presented in Figure 1 (where entry is defined at 7×10^6 feet altitude). The Venus entry velocities during these periods range from 40,000 fps to over 50,000 fps, while the Mars entry velocities are on the order of 22,000 fps to 26,000 fps. In the case of Mars entry, the tenuous atmosphere presents problems in providing for sufficient dissipation of an entry vehicle's initial energy by requiring low ballistic parameter ($M/C_D A$) vehicles and shallow entry angles. The high density Venusian atmosphere, on the other hand, is quite adequate for providing energy dissipation, but the high entry velocities introduce problems in managing the entry heating environment.

Figures 2 and 3 present the atmospheric pressures and densities for the upper, mean, and lower model atmospheres obtained from Reference 1. The corresponding pressures and densities for the ARDC 1959 earth atmosphere are dashed on the two figures for comparison. The Venusian model atmospheres are seen to be considerably denser than earth throughout the altitudes influencing entry. The effects of this, as will be illustrated



later in Figures 13 and 14, are that an entry vehicle will decelerate high in the Venusian atmosphere where experiment deployment can be considered at relatively low sink rates for relatively heavy payload packages.

ENTRY ENVIRONMENT

Although the high density atmosphere makes entry "easier" in some respects, the high entry velocities do present particular design problems. The ensuing entry environment becomes of considerable concern and could impose severe structural and heating penalties on the entry vehicle shell structure and payload. The entry environment, however, is a strong function of the vehicle characteristics and initial entry angle. For a light weight low ballistic parameter vehicle, deceleration would occur at low densities in the upper atmosphere where the radiation heat transfer coefficient is lowest. Radiation heat transfer from the shock layer is of particular interest for the high velocity Venus entries since it is a strong velocity as well as density dependent mechanism from which current ablation materials offer poor protection.

The initial entry angle is also important since shallow entry provides for more gradual slow down in the upper atmosphere resulting in lower deceleration and reduced radiation heating. The longer heating times associated with shallow angles, however, increase the convective heat load. For a given vehicle, a minimum heat load entry angle exists by trading off the radiation and convective heat loads. Generally, due to the sensitivity of radiative heating to entry angle, this minimum heating entry angle will tend to be relatively shallow for the high entry velocities of interest for Venus.

STRUCTURAL LOADS

The peak decelerations for a ballistic vehicle are presented in Figure 4 for entry into the low density Venus model atmosphere. Except for the shallow entry angles, the low density model has the highest effective scale height in the stratosphere resulting in the highest structural loads of the three model atmospheres. The loads for the shallow angles are presented in Figure 5 for entry at 49,000 fps.

If lift was introduced, the structural loads could be reduced, but at the expense of deeper penetration and potentially higher heating. A lifting vehicle would also require roll stabilization and a more complex vehicle structure. In fact, the lifting structure under the low loads could weigh more than the ballistic structure under the higher loads due to packaging

efficiency. Gee sensitive instrumentation might require low load considerations, but at this point it is felt that lifting entry is not necessary for unmanned systems, since the 100 gee's or so, Figure 5, for shallow entry should not penalize instrumentation appreciably.

Shallow entry could present some operational constraints, as will be discussed later, but, it does tie in with the desire to reduce the radiation heating, which is of considerable concern.

AERODYNAMIC HEATING

The maximum radiative and convective heating rates to the stagnation point of a one foot radius spherical nose are presented in Figure 6 for an entry velocity of 49,000 fps utilizing the low density atmospheric model. The corresponding integrated heating loads are presented in Figure 7. The radiation load was computed from a correlation for $\text{CO}_2\text{-N}_2$ mixtures² and was assumed to originate in an optically thin adiabatic shock layer. Recent studies^{3,4} have found that this correlation overestimates the heat transfer by a factor of two or three since it does not account for the energy absorption within the shock layer. The absolute magnitude of the radiative heating is, therefore, in question, but the sensitivity to parameters is significant. The important point is the effect of entry angle and ballistic parameter which is illustrated by the exponents on the variational functions in Figures 6 and 7.

Of particular concern under the high radiation heating is the performance of ablator materials. Subsurface heating from ultraviolet radiation can increase internal gas pressures resulting in surface spallations. Combined with shear forces in the boundary layer, severe mechanical failure of the material can result. Also, the effective heat protection capabilities of ablators under high radiation load is not well understood. The large blockage of convective heating due to transpiration of the products of ablation in the boundary layer has a negligible effect on the radiation heating. Low effective heats of ablation are then assumed under radiation loads, resulting in larger quantities of ablator loss during entry.

As an additional consideration, the high shear stresses on the surface material dictate high stress, high density ablator materials. These materials have characteristically higher thermal conductivity and, therefore, greater insulation weight requirements in order to maintain reasonable bond line temperatures.

VEHICLE CONSIDERATIONS

Figures 6 and 7 deal with the stagnation point heating. The heating penalties to the entire entry vehicle are more complex and depend upon the vehicle shape. Generally, blunt shapes minimize convective heating and slender shapes minimize radiation heating. This is based on the dimensional dependence of convective and radiative unit area heating. The convective dependence varies as $1/\sqrt{R}$ and the radiative heating as R (R is the vehicle spherical nose radius). However, a recent paper¹⁰ concludes that there is a weaker dimensional dependence of radiation due to shock layer absorption, and that radiation varies more like \sqrt{R} . In the interest of conservatism, though, Figure 8 is based on the stronger dimensional dependence of radiation.

With a given set of entry conditions, an optimum vehicle shape can be generated, theoretically, to minimize the total heat load and heat protection weight. This optimum vehicle is difficult to generate, however, due to the coupling of the radiation and convective mechanisms, ablator performance and the uncertainties of turbulent transition in a boundary layer contaminated with products of ablation, and does not lend itself readily to parametric analysis. These effects are currently subjects which are receiving considerable attention from theoretical and experimental researchers.

Rather than undertake the task of optimizing entry vehicle shapes for a variety of entry conditions, a blunted cone with a 60° half angle and spherical nose radius ratio of 5 or so will be considered here. The 60° cone has a large hypersonic drag coefficient and, therefore, a characteristically low ballistic parameter required to accommodate the high Venusian entry velocities. The 60° blunted cone will be considered as a nominal configuration as long as the payload can be reasonably packaged without exceeding some base diameter, say 20 ft. Alternatively, a more slender, higher fineness ratio cone could be employed. Although a more slender cone would have the additional feature of reducing the radiation heating penalty, the radiation load could be more than off-set by turbulent heating.

In order to keep probe designs as tenable as possible, then, entry will not be considered for very steep entry unless the vehicle is dimensionally small and light weight.

With shallow entry in mind, typical payload fractions are presented in Figure 8 for the 60° cone entering Venus at 49,000 fps at an entry angle of -13° . The -13° angle is the steep side of the entry corridor which will be discussed later.

For a given diameter in Figure 8, the fall off in payload fraction at the low ballistic parameters results from large structural and thermal insulation weights, while at the high ballistic parameters the fall off is due to large radiation heating loads. The dimensional dependence of radiation shows up by reducing the mass fraction at the larger diameter .

These payload fractions can then be used as a guide for determining entry probe capabilities.

ENTRY CORRIDOR

The entry corridor is generally defined as the difference between the hypothetical vacuum periapsis altitudes of two entry trajectories with specified operational constraints. The absolute overshoot of the entry corridor, although not necessarily the operational overshoot, can be thought of as the trajectory which enters at a shallow angle but does not exit the atmosphere following initial entry. For the Venus entries, the flight path angles corresponding to the absolute overshoot are presented in Figures 9 and 10. It is evident from Figure 11 that entry near the absolute overshoot produces large range dispersions over the planet surface. Since presently there are no surface features on Venus which require accurate targeting, range dispersions should not represent an appreciable constraint. Entry angles of -11° to -12° will then be considered tolerable for operational overshoot limits.

Since the primary motivation for maintaining the angles shallow is the high heating loads at steep angles, the steep side of the corridor will be determined by the capability of the approach guidance system. For guidance corridor capability on the order of 10 nautical miles, the undershoot can be maintained at about -13° . With a -12° overshoot, the resulting 1° corridor has a 4° to 5° planetary central angle dispersion over the estimated range of atmospheric uncertainty (Figure 11).

Although the corridor constraints are somewhat heuristic, little would be gained operationally by opening up the steep side of the corridor only a few degrees. This will be illustrated later under operational considerations.

ATMOSPHERIC OPERATIONS

As discussed previously, the high density structure of the Venusian atmosphere offers a certain amount of compensation for the high entry velocities and high atmospheric temperatures.

The temperature profiles for the three model atmospheres' are presented in Figure 12. It is apparent that the thermal environment throughout the lower levels of the atmosphere will be a fundamental design constraint for any operational system. There is an intermediate region offering "temperate" conditions, however, which is of great exploratory interest occupying an altitude band from 125,000 ft. to 215,000 ft. and ranging in temperature from 0°F to 100°F. This region, shaded in Figure 12 could offer a hospitable environment for conducting atmospheric experiments and searching for life forms.

The temperate region lies below the estimated tops of the dense Venusian clouds, and hence, considerable uncertainty exists as to its structure. No credibility is implied here, but one must work with what appears to be the best available data.

Therefore, with the present models¹ it is of interest to pursue the temperate region further.

The equivalent earth density altitudes in this region are on the order of 40,000 ft. or lower. With these relatively high densities, flotation devices could be considered as reasonable exploration platforms. Unfortunately, a constant buoyancy device could not guarantee flotation within this "temperate" region with the large density uncertainties that presently exist. For example, the darkened circles on Figure 12 represent the operational conditions for a constant buoyancy device constrained not to violate an upper temperature limit of 100°F. The darkened triangles are constrained to an upper temperature limit of 200°F. In both cases, the mean model atmosphere is within the temperate region. However, when atmospheric extremes are considered, the latter case has a possible temperature range of -80°F to +200°F, and the former -120°F to 100°F. The -80°F to +200°F range is more compatible with nylon balloon material performance,⁶ but the higher temperatures could be quite penalizing to experiments and electronic systems.

It appears reasonable to expect that the present uncertainties in the Venusian atmosphere should be reduced following the 1967 Mariner. It is not clear, however, that the density and temperature uncertainty will be reduced sufficiently to accommodate a constant buoyancy device. At least some type of altitude cycling floater, or variable buoyancy device, would be desirable for providing wide altitude coverage and sufficient flexibility to compensate for atmospheric uncertainties and to provide for deeper soundings if a more hospitable environment is discovered on site.

TERMINAL VELOCITY

In Figure 13, the "terminal" velocity is presented for a ballistic parameter of 1 slug/ft^2 . The "terminal" velocity is the quasi steady state sink rate at a given altitude under the influence of the Venusian gravity, and varies as the inverse square root of the ballistic parameter ($m/C_D A$). The altitudes and times to achieve terminal velocity are presented in Figure 14 for the 49,000 fps entry velocity, and show that the quasi steady state sink rates occur at quite high altitudes. Following terminal velocity, the corresponding times to descend between altitudes at these sink rates are presented in Figure 15. It is apparent that there can be as much as one hour uncertainty in the time to descent to the planetary surface for a vehicle with a ballistic parameter of 1 slug/ft^2 , and considerably more uncertainty for a very low ballistic parameter parachute descent.

A ballistic parameter of 1 slug/ft^2 is used here for convenience since most of the parameters scale appropriately. The ballistic parameter of an entry vehicle, though, will not be the same at hypersonic and subsonic speeds. In addition, some form of transonic stability augmentation will probably be required for any blunt based cone. A drag chute is quite effective in this respect, and will also change the ballistic parameter.

REACHING THE TEMPERATE REGION

With the present atmospheric models in mind, it is of interest to determine the feasibility of delivering a flotation device to the temperate region. An unmanned probe ($m/C_D A = 1 \text{ slug/ft}^2$) entering the Venusian atmosphere during the 1978 dual-planet flyby ($V = 49,000 \text{ fps}$) at the undershoot of the entry corridor ($\gamma = -13^\circ$) would achieve "terminal" conditions at an altitude no lower than 130,000 ft., approximately 170 seconds after entry. This is illustrated in Figure 14 based on the low density (worst case) model.

When terminal conditions are achieved, i.e., when approximately $1 g_\oplus$ is sensed on-board, a flotation device would be deployed and the inflation process begun. Since the dynamic pressure corresponding to an $m/C_D A = 1 \text{ slug/ft}^2$ under

terminal conditions is on the order of 30 psf, utilizing nylon for the balloon material would eliminate the need for a large retardation parachute. Only a small supersonic device would then be needed for transonic stability. Various nylon devices have been successfully deployed under prolonged dynamic pressures exceeding 30 psf. Hot gas bag balloons and various paraglider configurations are examples.

With a small supersonic parachute, deployed to maintain transonic stability and providing a total system subsonic $m/C_D A = 1 \text{ slug/ft}^2$, it would take approximately 4 minutes (minimum) to descend from 130,000 feet to 80,000 feet altitude. (80,000 feet in the low density model corresponds to a temperature of 350°F which is an intermittent operational limit for nylon material⁶.) During the descent, data could be gathered and the time could be used to deploy and inflate a balloon for flotation. Following the inflation period, the balloon system would ascend to the temperate region for operations.

Since descent time would actually be increased with the drag area of the inflating balloon the vehicle would never reach such a low altitude. Also, as an alternate procedure for large slow filling balloons, a large subsonic parachute could be employed to increase the descent time by as much as a factor of 10.

It is quite reasonable, then, to consider "targeting" for this temperate band.

OPERATIONAL CONSIDERATIONS

The requirement for shallow entry does present operational constraints. An entry probe entering at shallow angles may be out of view of the flyby spacecraft due to the curvature of the approach trajectory and the large central angle between the entry point and the approach asymptote. To illustrate this, data for the 1975 single-planet twilight flyby geometry is available and is used as an example.⁷ The energy associated with the 1975 single-planet flyby is considerably less than some of the multi-planet flyby missions, but the geometry does reveal some of the operational considerations.

There is a singular relationship between the entry angle imposed on an entry probe and the position of the entry point measured on the planet surface from the spacecraft periapsis. This relationship is presented in Figure 16 for the 1975 single-planet twilight flyby. With a minimum differential

anomaly of 90° required for visibility between the probe at entry and the spacecraft on the approach asymptote, the entry point must be located at an anomaly of 45° or greater. This would increase to 50° if 5° minimum look angle was imposed. With the entry point at an anomaly of 45° , then, the probe would enter at an entry angle of -32° which exceeds the previously discussed corridor constraint by 20° and would result in severe heating penalties.

Some adjustment can be made to the entry angle and anomaly relationship on Figure 16, but it becomes quite costly in terms of propulsion.⁷ The approximate parameter sensitivities indicated on Figure 16 result in about a 300 ft. per second ΔV per degree entry angle to reduce the entry angle at a constant anomaly angle. In addition, this ΔV practically all goes into increasing the trajectory energy and, therefore, entry velocity. Thus, it is too impractical to reduce the entry angle propulsively in order to maintain a constant anomaly for entry point visibility to the spacecraft on the approach asymptote, i.e., a long time before periapsis passage.

This entry angle/anomaly angle relationship should also be kept in mind in the case of reducing the trajectory energy in order to provide for a lower entry velocity. When the entry velocity is reduced, the entry angle will steepen at a given anomaly. Entry angle steepening is reduced, though, if the impulse is applied near entry. In any event, the propulsive ΔV would have to be greater than or equal to the required entry velocity reduction.

The implications are, therefore, that the entry point for large entry probes (small, low ballistic parameter atmospheric probes excluded) will not be visible to the spacecraft for a very long time before the spacecraft passes periapsis. An idea as to just how long can be obtained from the times before periapsis passage for different spacecraft anomaly locations presented in Figure 14. Thus, for a -12° entry angle, the spacecraft would not acquire line of sight to the probe (post entry) until about 105° or 1.5 hours before periapsis, assuming the probe entry point is in the plane of the spacecraft flyby. Out of plane entry points will be even more restriction. For direct communication between probe and spacecraft, a typical probe would require on the order of an hour lead on the spacecraft.

The conclusions to be drawn are that the spacecraft will be able to communicate to the probes and receive data transmissions for relatively short periods during the planetary encounter. It appears, then, that for longer data transmission periods, an orbiting vehicle will have to be tied into the data link. The

actual penalties will require more detailed analysis with actual payloads and entry probe ballistic parameters in mind.

AREAS OF INTEREST

As an additional consideration, certain areas on Venus could require some degree of targeting in order to investigate localized conditions. Several of these areas exist due to the slow rotational rate of the planet.

Since Venus rotates very slowly on its axis, one side of the planet faces the sun for long periods while the other side is occulted. The solar energy absorbed in the atmosphere on the sunny side will then be the working energy for the atmospheric circulation patterns. It is postulated that this circulation can be described as a source-sink flow diverging from the sub-solar point and flowing circumferentially to the anti-solar point.⁹ In addition, prolonged heating of the sub-solar region could result in localized atmospheric and surface phenomena. On the other hand, the Venusian poles receive sunlight at very skewed angles and could actually harbor surface temperature considerably lower than indicated in Figure 12. With these considerations in mind, then, the four points, i.e., sub-solar, anti-solar, North Pole, and South Pole could represent areas of scientific and exploratory interest.

Three flyby missions were investigated to determine the relative positions of these four points to the flyby geometry.⁸ The results are presented in Table 1. The anomaly angle is measured from the flyby periapsis to the approach asymptote, although in general, not in the plane of the flyby. The entry angle is the approximate angle a probe would enter at to reach the specific point. The visibility angle is measured above the local horizontal at the point of interest to the approach or departure asymptote of the flyby spacecraft.

Some conclusions can be drawn for the two multi-planet missions. For the 1977 mission, the sub-solar point can be investigated with a large probe on the first encounter while the anti-solar and North Pole would have to wait until the second encounter. Poor visibility of the sub-solar and anti-solar points would permit short transmission times, while the North Pole has excellent visibility during departure.

In 1978, the anti-solar and North Pole are again accessible with a large probe, but the anti-solar point will require a very shallow entry.

The South Pole has poor accessibility throughout the years, although very shallow entry in the 1977 first encounter and 1978 missions could put a probe in its proximity.

For the 1975 single-planet flyby, the relatively low entry velocity (36,000 fps) would permit the investigation of all the points of interest, although only the anti-solar point on departure would be visible.

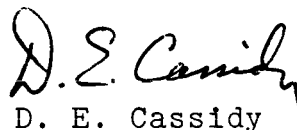
CONCLUSIONS

An attempt has been made to point out some of the considerations for unmanned entry into the Venusian atmosphere during a number of the manned flyby missions in the late 1970's. While the high density structure of the Venusian atmosphere almost certainly guarantees successful entry in terms of energy dissipation, the high entry velocities penalize entry vehicle designs and dictate shallow entry corridors resulting in restrictive operational capability. The operational restrictions limit point targeting and direct data transmission from probes to the flyby spacecraft. For large probes, the data transmission times would be limited to on the order of 1.5 to 2 hours during the busy planetary encounter period.

Small increases in the entry angle could be tolerated in terms of the entry heating environment, but in most cases would have negligible effect on the operational constraints.

The high density structure of the Venusian atmosphere results in low rates of sink at high altitudes. This produces large dispersions in time to fall due to uncertainties in the atmospheric density, but permits high altitude deployment of payloads.

It is quite reasonable to target for the temperate region where temperatures are on the order of 0°F to 100°F. Due to the present uncertainties in the atmosphere, though, a constant density flotation device can not be used.


D. E. Cassidy

1013-DEC-nmm

Attachments

References 1-9
Figures 1-17
Table I

REFERENCES

1. "Space Environment Criteria Guidelines for Use in Space Vehicle Development," NASA TM X-53142, Robert E. Smith, Editor, dated September 30, 1964.
2. "Aerothermodynamics of Planetary Entry," Spiegel, J. M., Wolf, F., and Horton, T., Jet Propulsion Lab, Solar Probe Spacecraft, Report SPS 37-22, Vol. IV, Sec. 354, dated August 31, 1963.
3. "Study of Heat Shielding Requirements for Manned Mars Landing and Return Missions Summary Report," Lockheed Missiles and Space Company, NASA CR-308, dated October, 1965.
4. "Earth Entry at Hyperbolic Velocities," North American Aviation (SIA) Presentation at the Hypervelocity Reentry Research Review, Ames Research Center, May 22 and 23, 1967.
5. "Aerodynamic Heating of Conical Entry Vehicles at Speeds in Excess of Earth Parabolic Speed," NASA TR R-185, H. J. Allen, A. Seiff, and W. Winovich, dated December, 1963.
6. Discussion with Representatives of G. T. Schjeldahl Company.
7. "1975 Venus Lightside Flyby Trajectory of Spacecraft and Probes," Memorandum for File, Case 233, by J. J. Schoch, dated June 7, 1967.
8. Based on Unpublished Data from C. L. Greer, Bellcomm, Inc.
9. "A Discussion of the Deep Circulation of the Atmosphere of Venus," by R. M. Goody and A. R. Robinson, The Astrophysical Journal, dated November, 1966.
10. "Convective and Radiative Heat Transfer During Superorbital Entry," H. Hoshizaki, and K. H. Wilson, AIAA Journal, dated January, 1967.

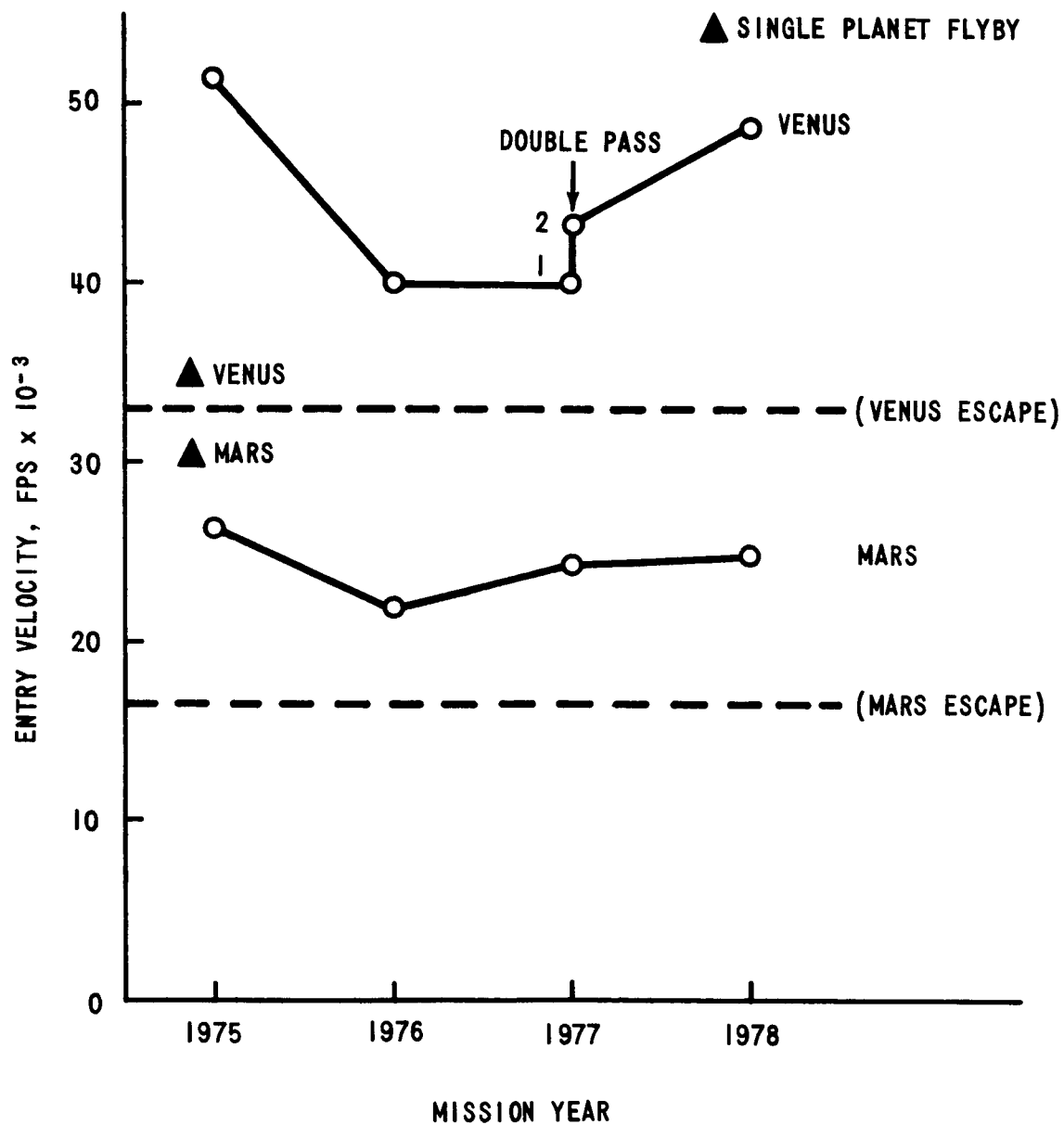


FIGURE 1 MARS-VENUS MULTI PLANET FLYBYS - BALLISTIC ENTRY VELOCITIES AT 7×10^5 FEET

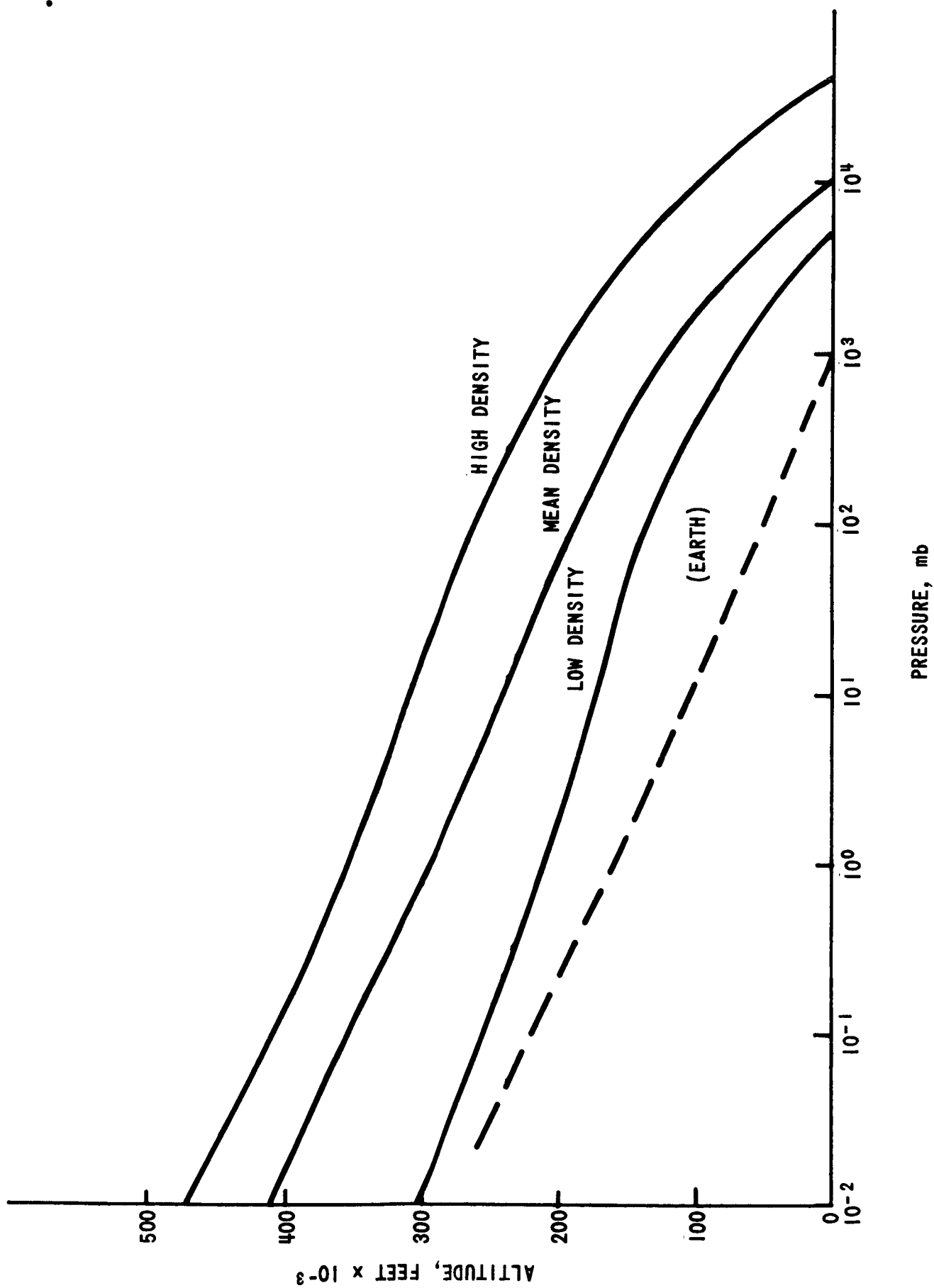


FIGURE 2 VENUS ATMOSPHERE, PRESSURE

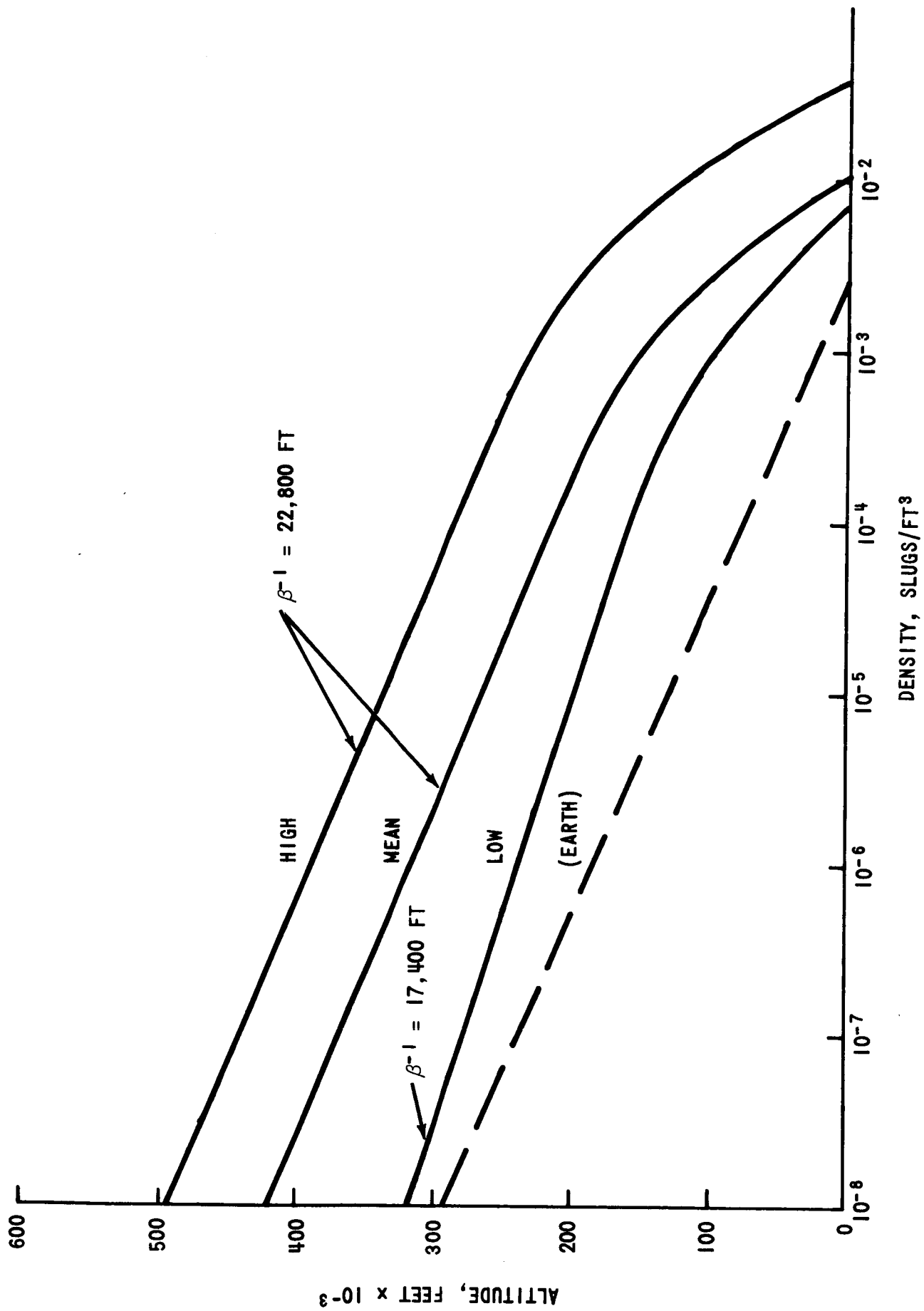


FIGURE 3 VENUS ATMOSPHERE , DENSITY

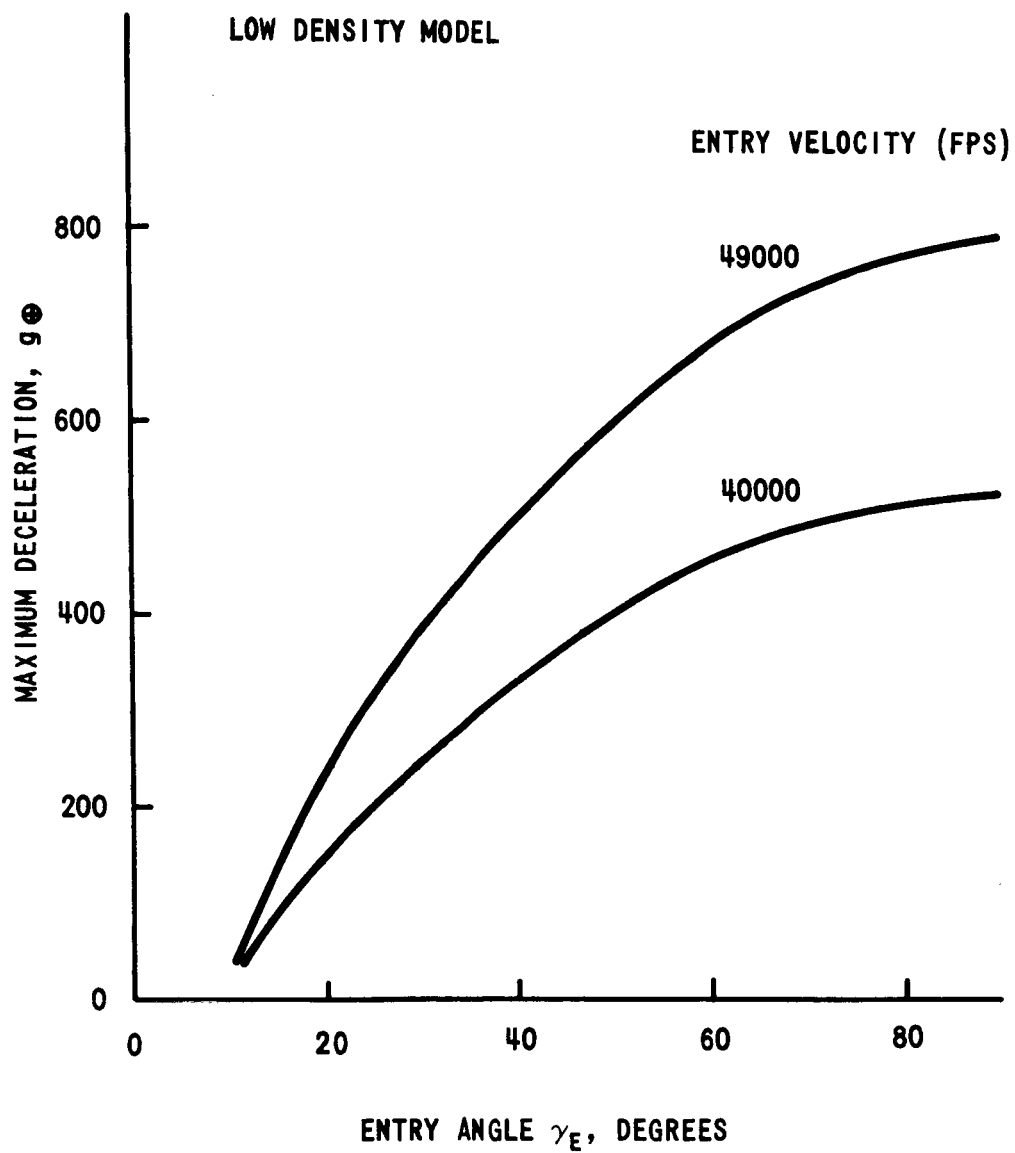


FIGURE 4 MAXIMUM DECELERATION, VENUS ENTRY

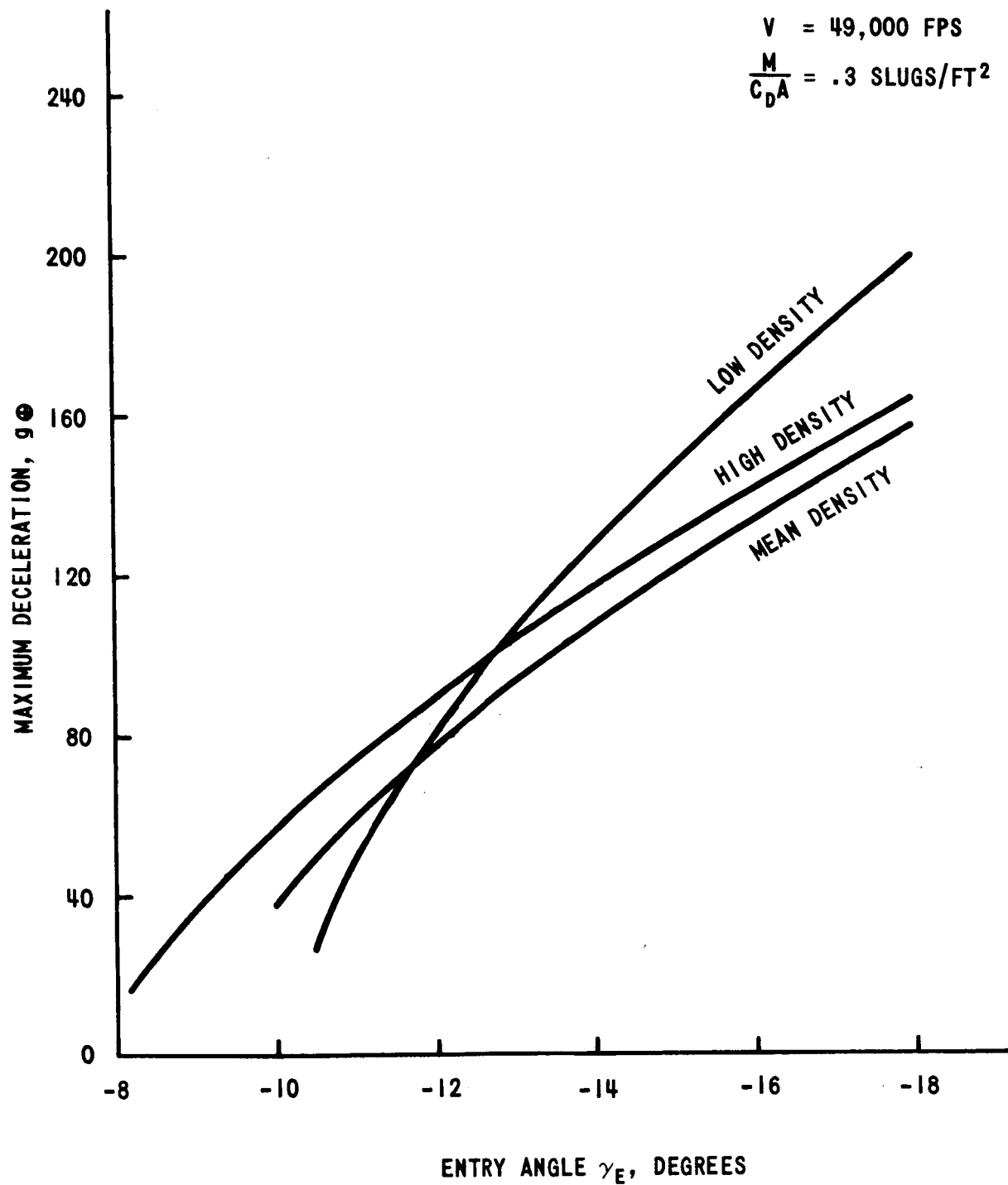


FIGURE 5 MAXIMUM DECELERATION, VENUS ENTRY

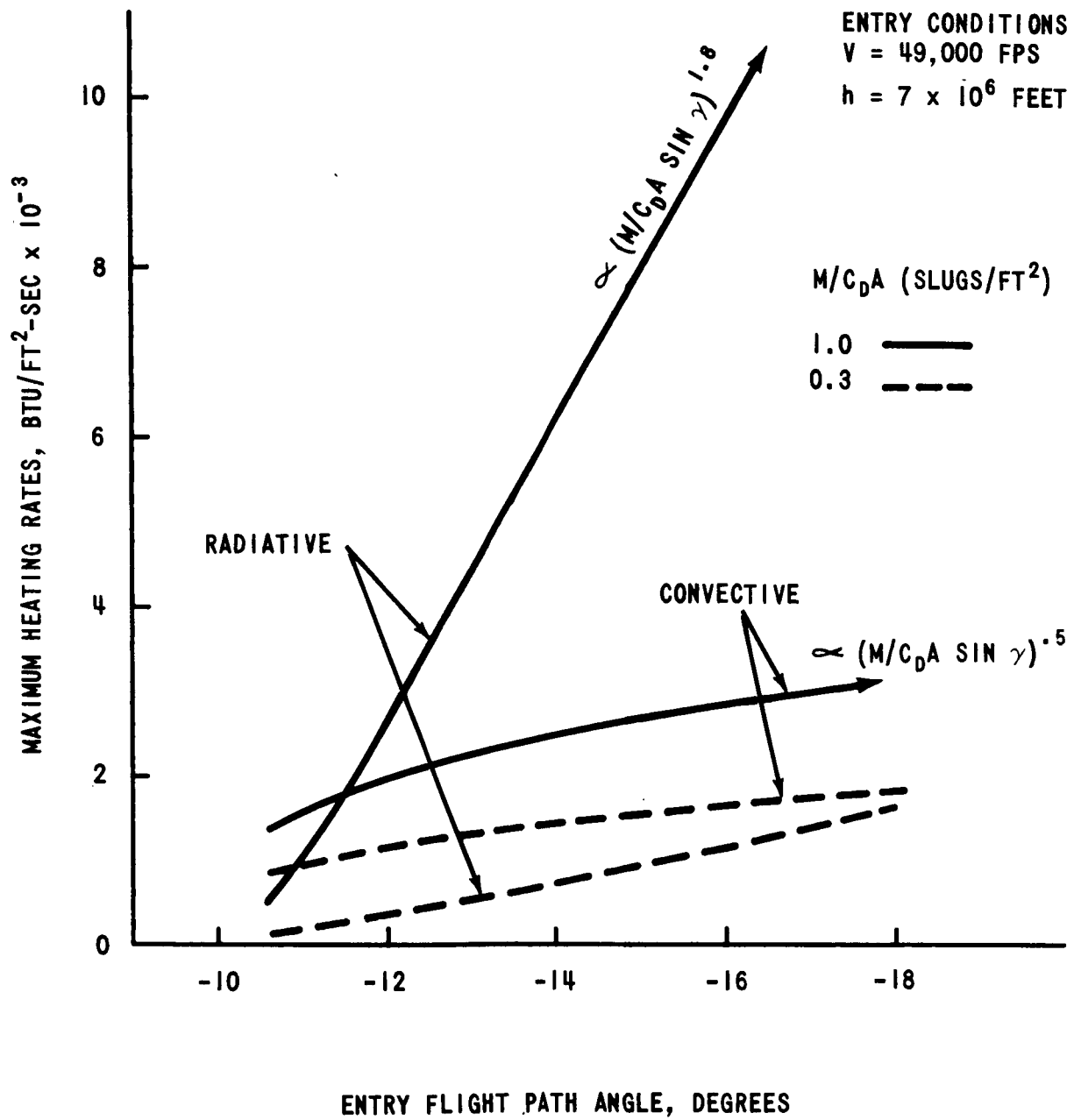


FIGURE 6 MAXIMUM RADIATION & CONVECTIVE HEATING RATES TO ONE FOOT RADIUS SPHERICAL NOSE, VENUS LOW DENSITY MODEL

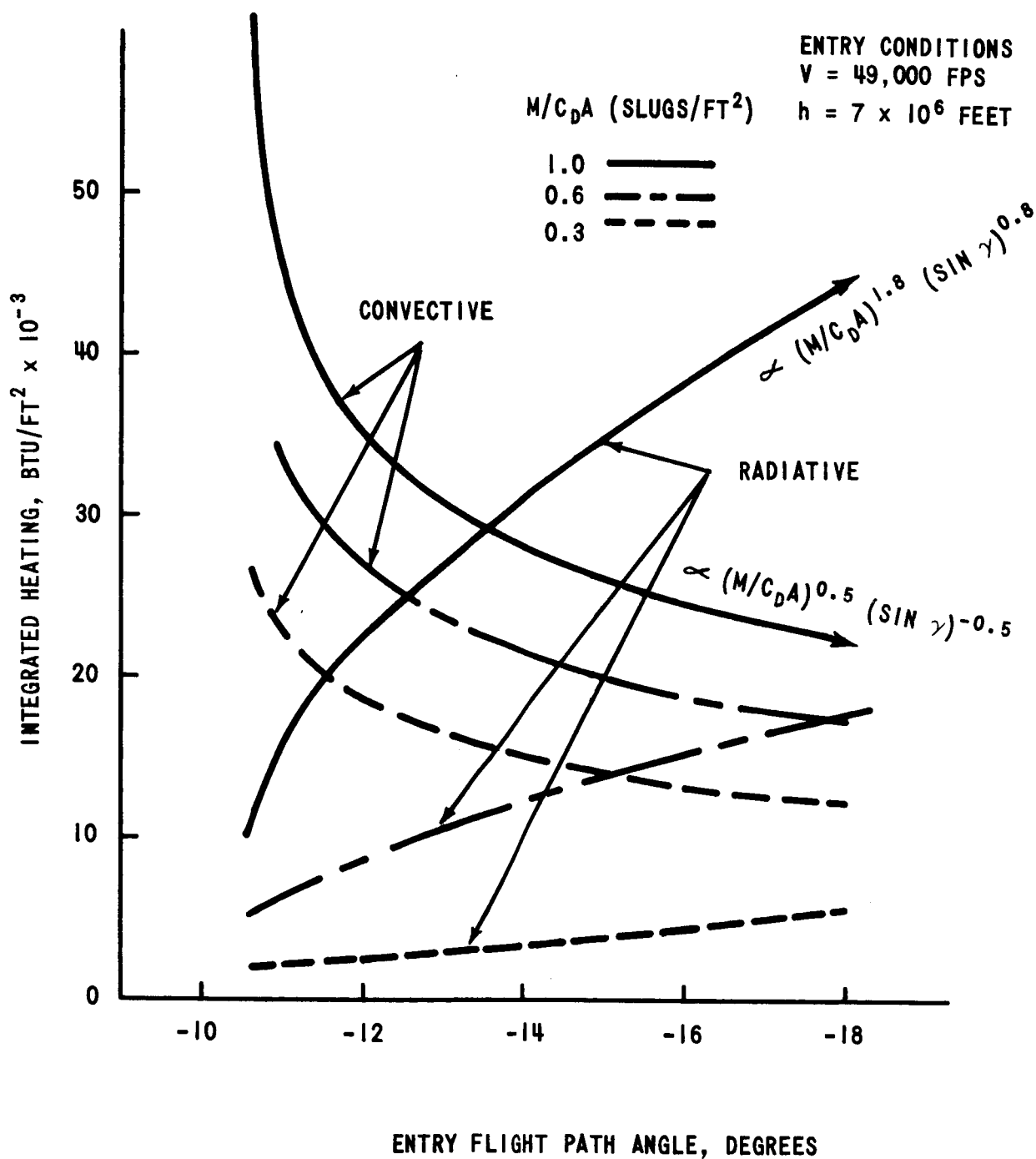


FIGURE 7 INTEGRATED HEAT LOAD TO ONE FOOT RADIUS SPHERICAL NOSE, VENUS LOW DENSITY MODEL

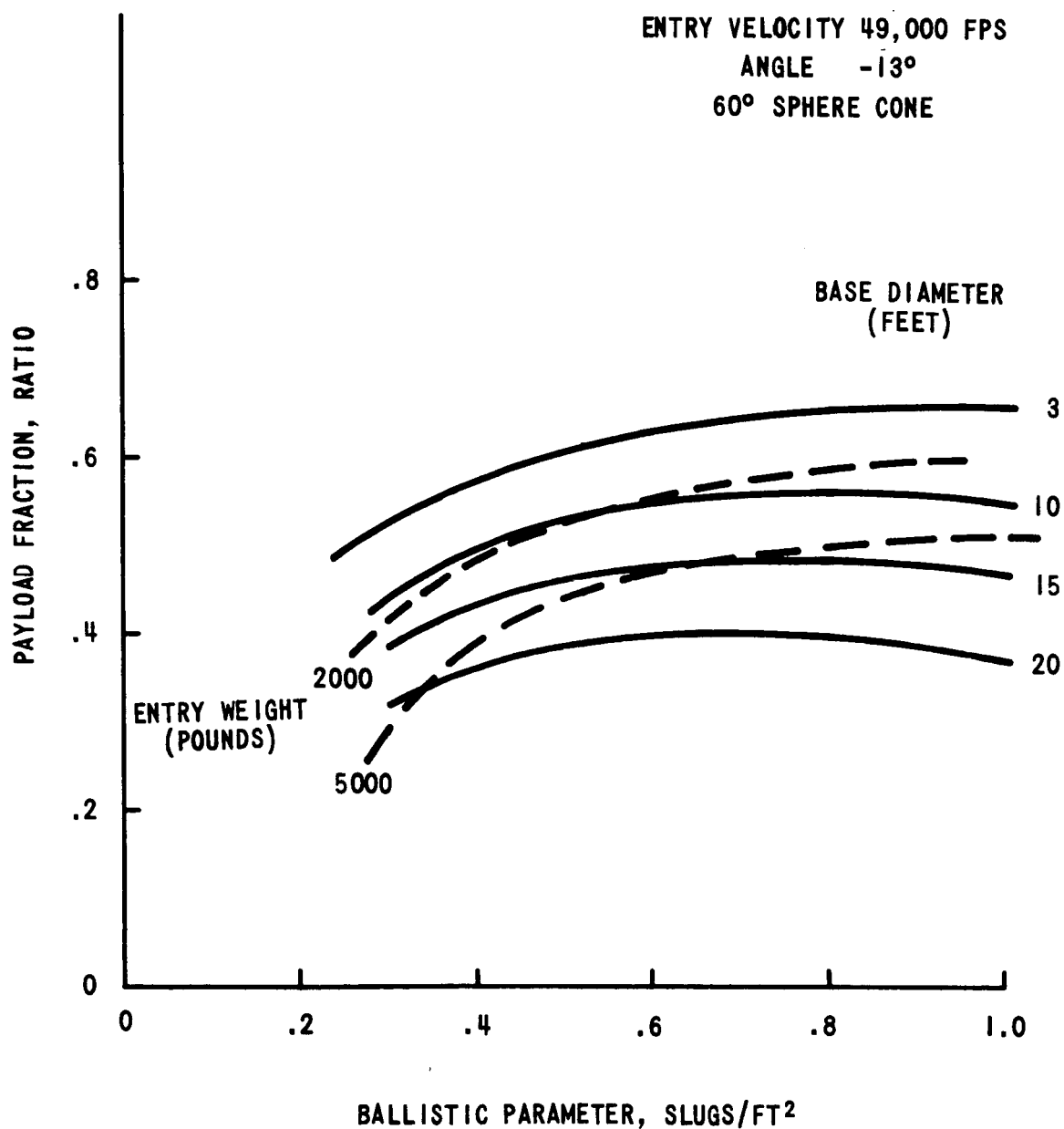


FIGURE 8 PAYLOAD-TO-ENTRY WEIGHT RATIO, VENUS BALLISTIC ENTRY

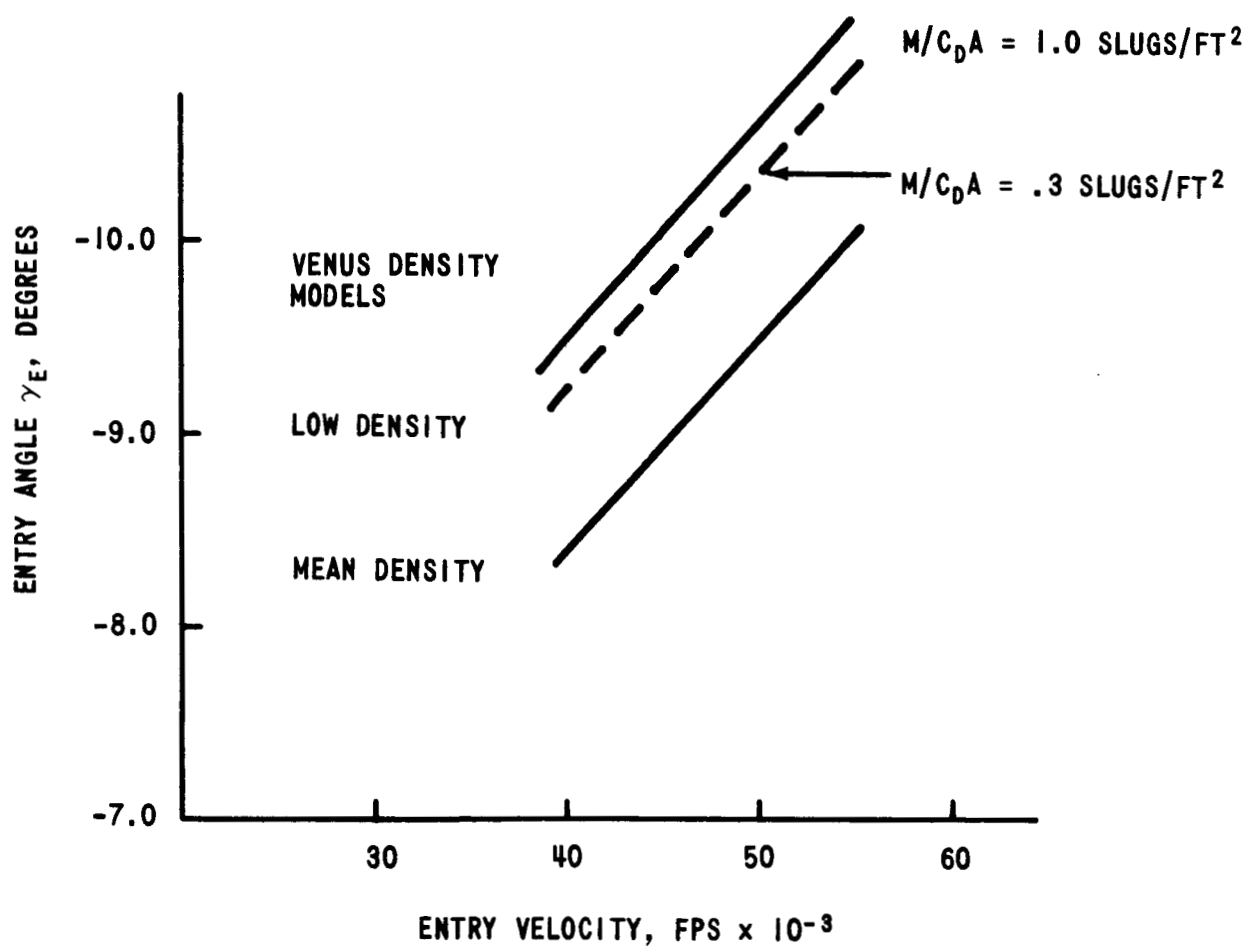


FIGURE 9 OVERTHROOT FLIGHT PATH ANGLE AT 7×10^5 FEET, VENUS BALLISTIC ENTRY

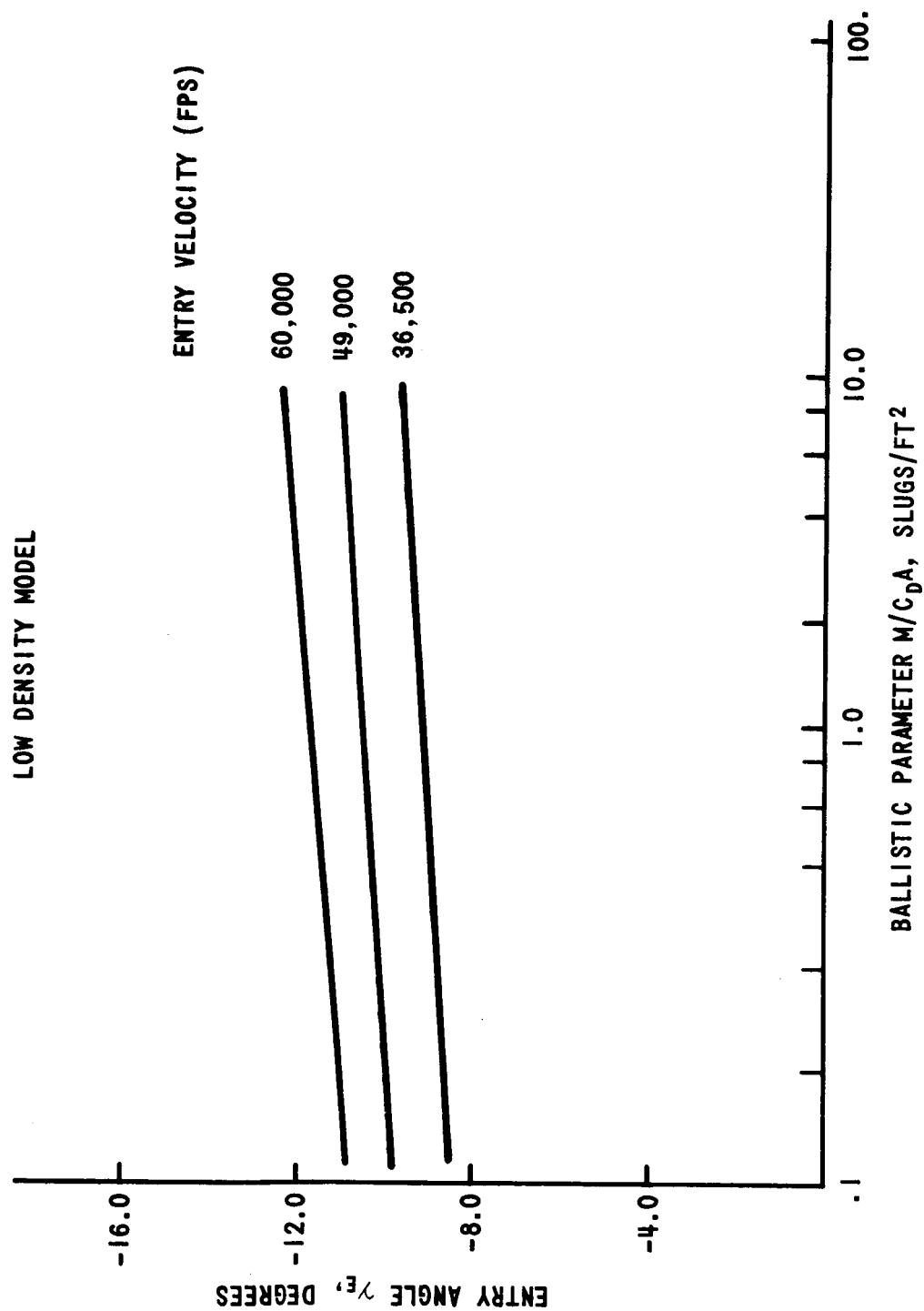


FIGURE 10 OVERSHOOT FLIGHT PATH ANGLE AT 7×10^5 FEET, VENUS BALLISTIC ENTRY

RANGE DISPERSION FOR VENUS ENTRY

$V = 49,000 \text{ FPS}$
 $M/C_D A = 1. \text{ SLUG/FT}^2$

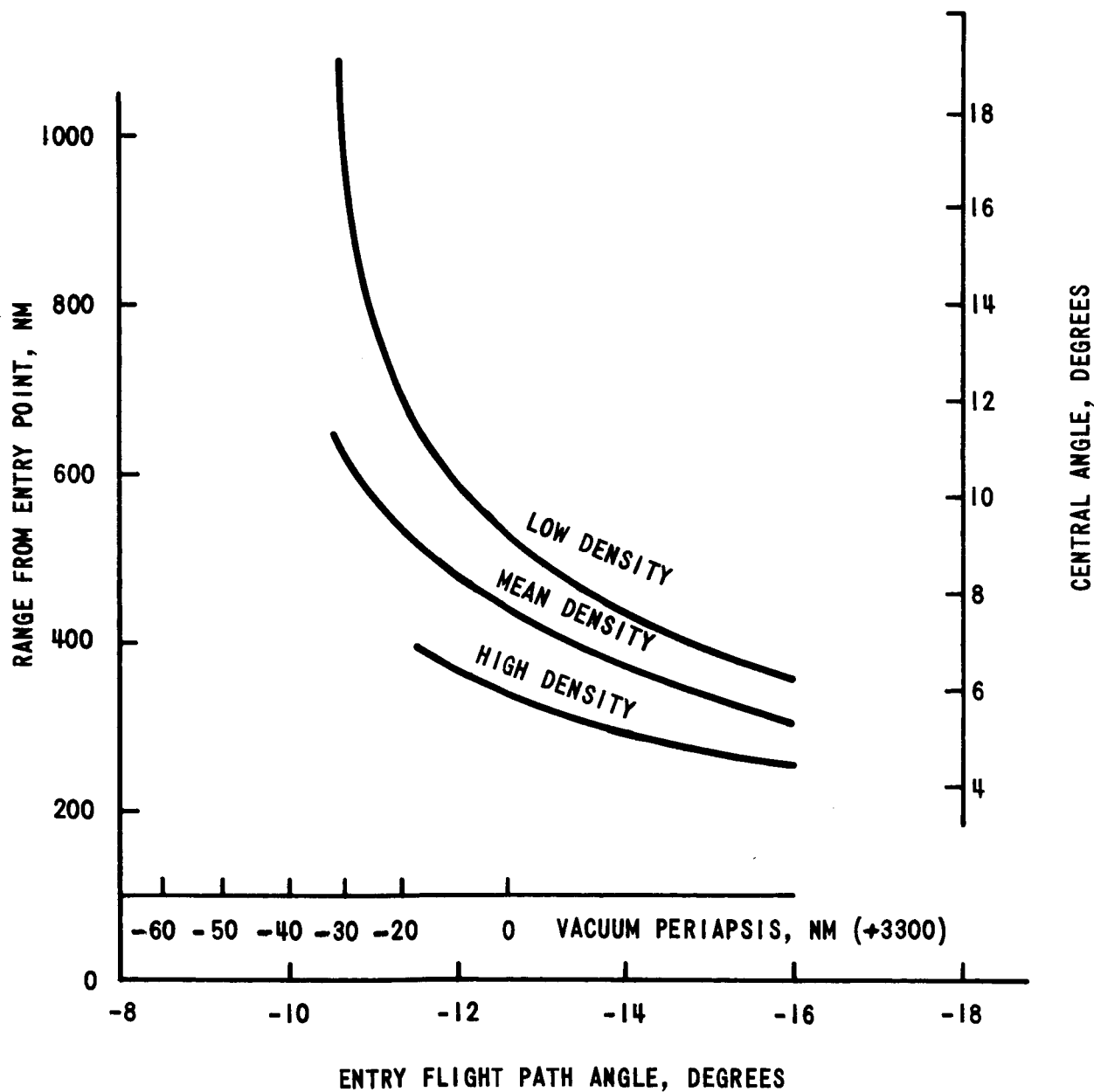


FIGURE 11 RANGE DISPERSION FOR VENUS ENTRY

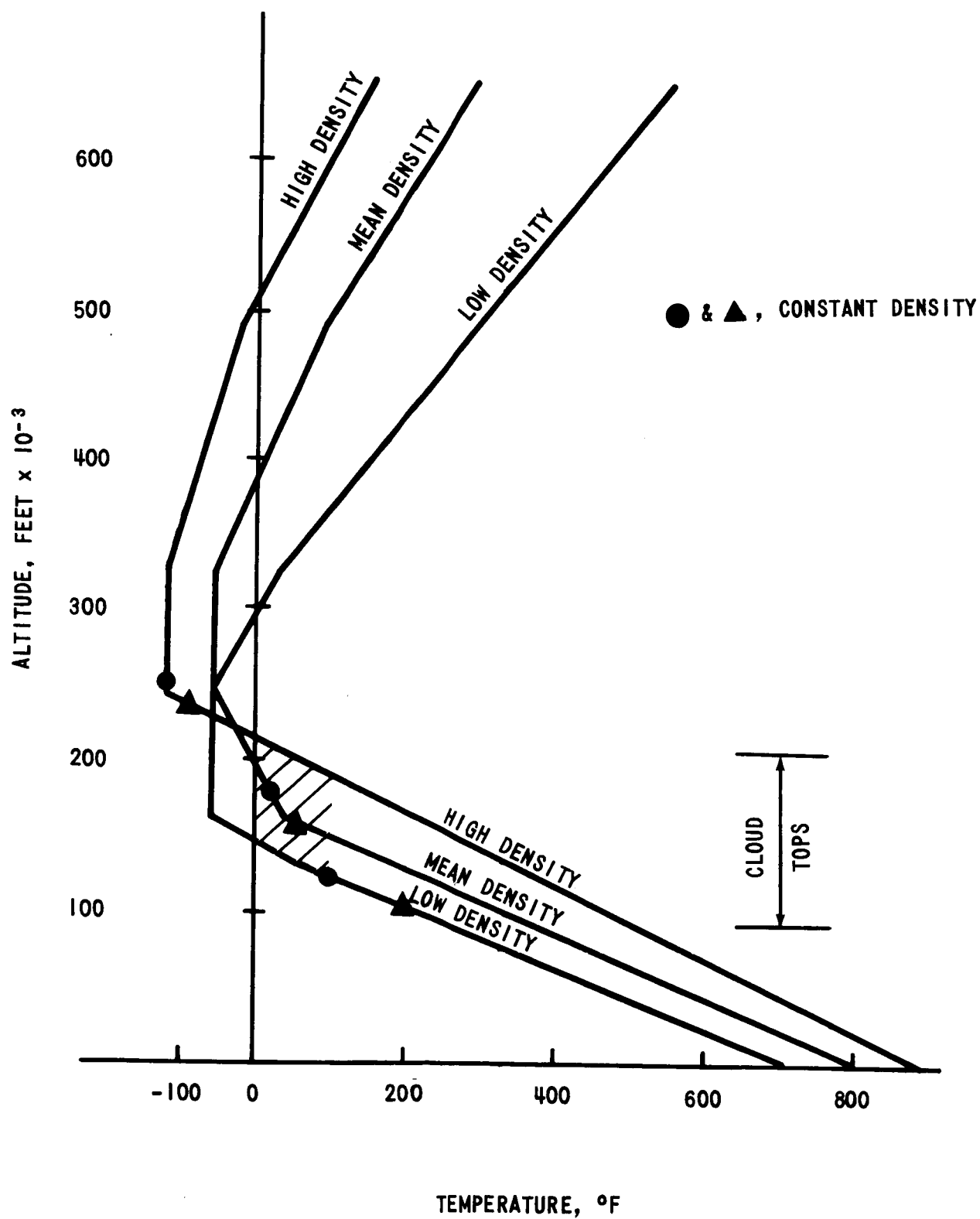


FIGURE 12 VENUS ATMOSPHERE, TEMPERATURE

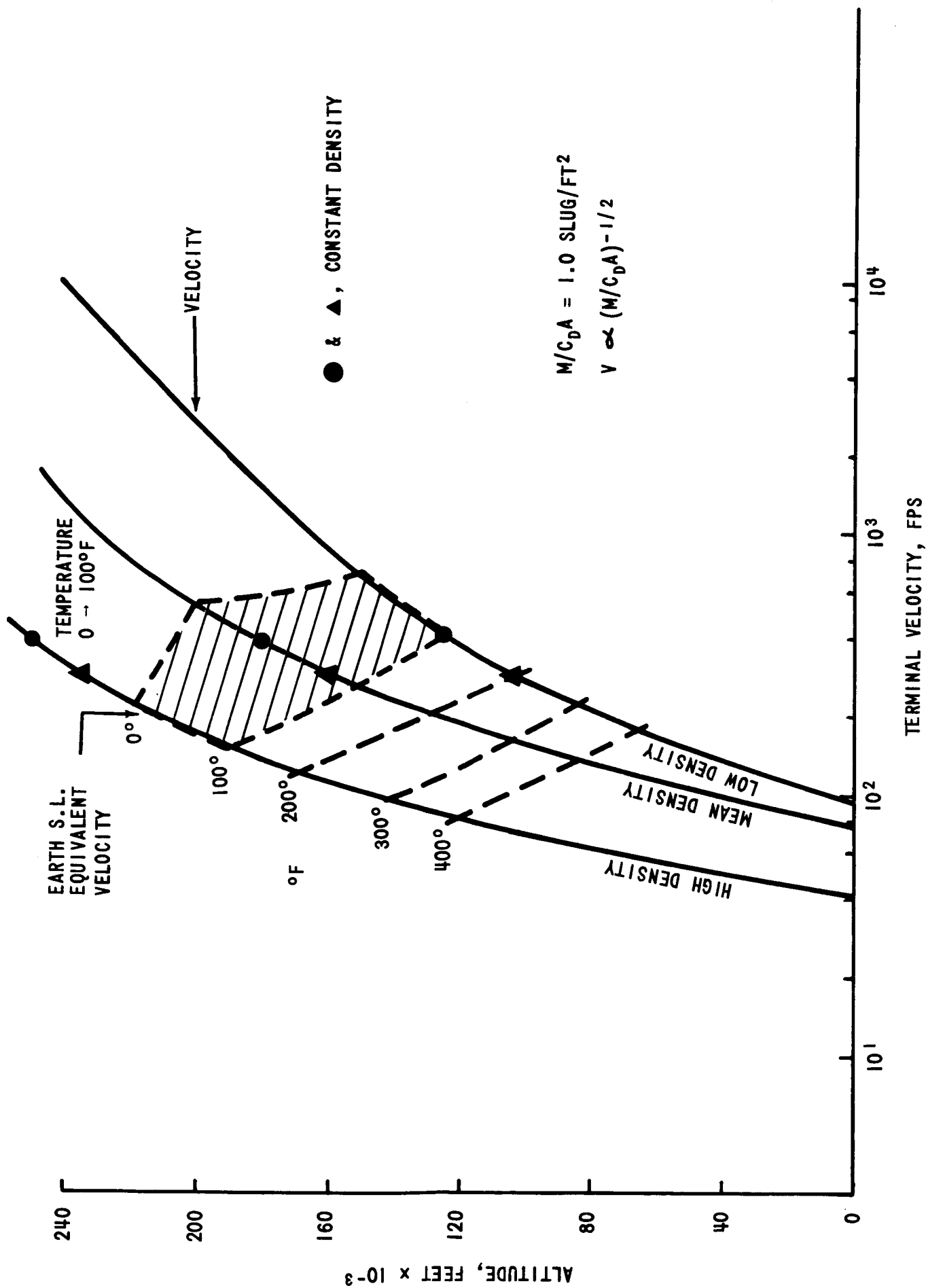


FIGURE 13 "TERMINAL" VELOCITY IN VENUS MODEL ATMOSPHERES

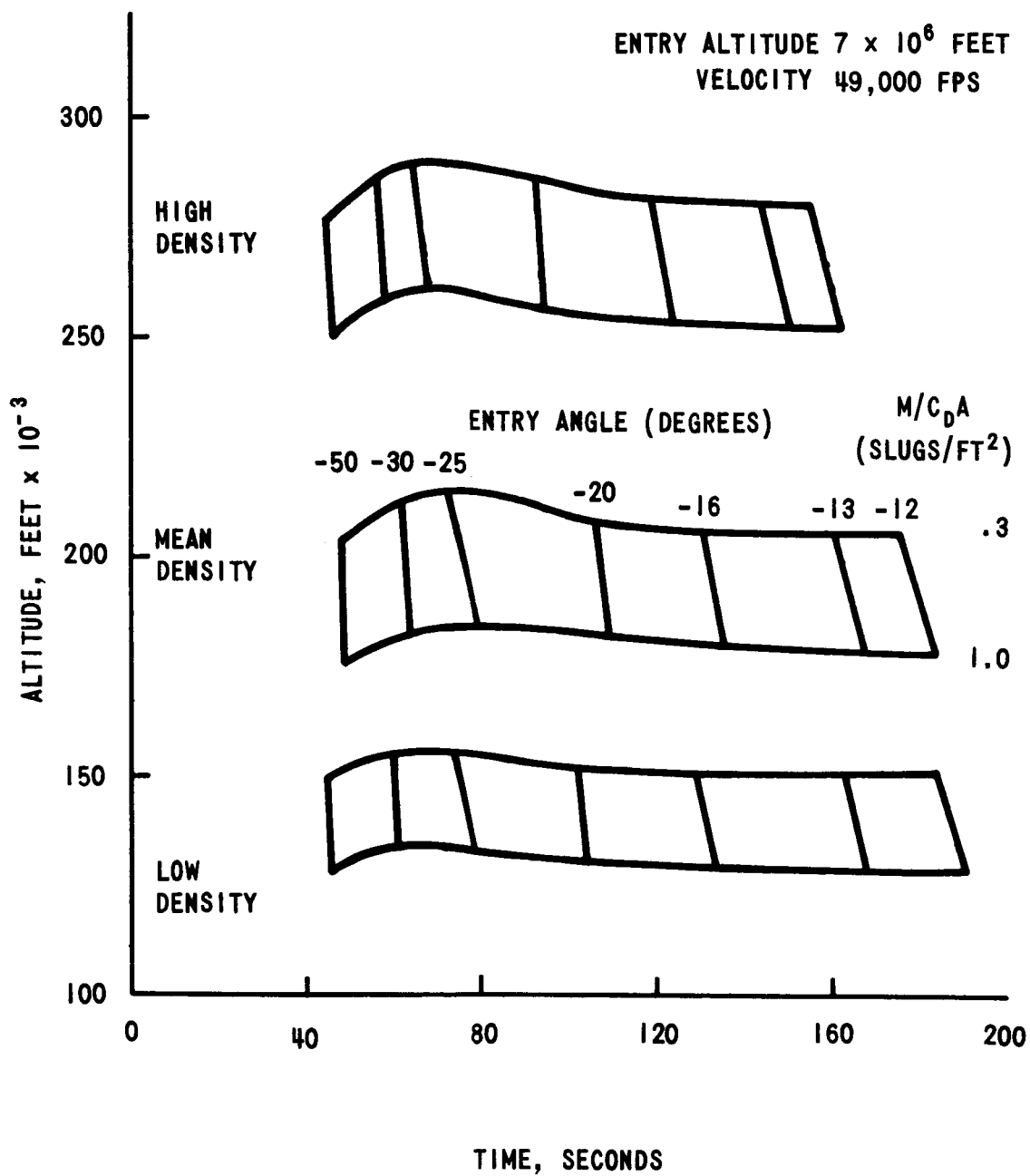


FIGURE 14 ALTITUDE vs. TIME-TO-ACHIEVE TERMINAL VELOCITY

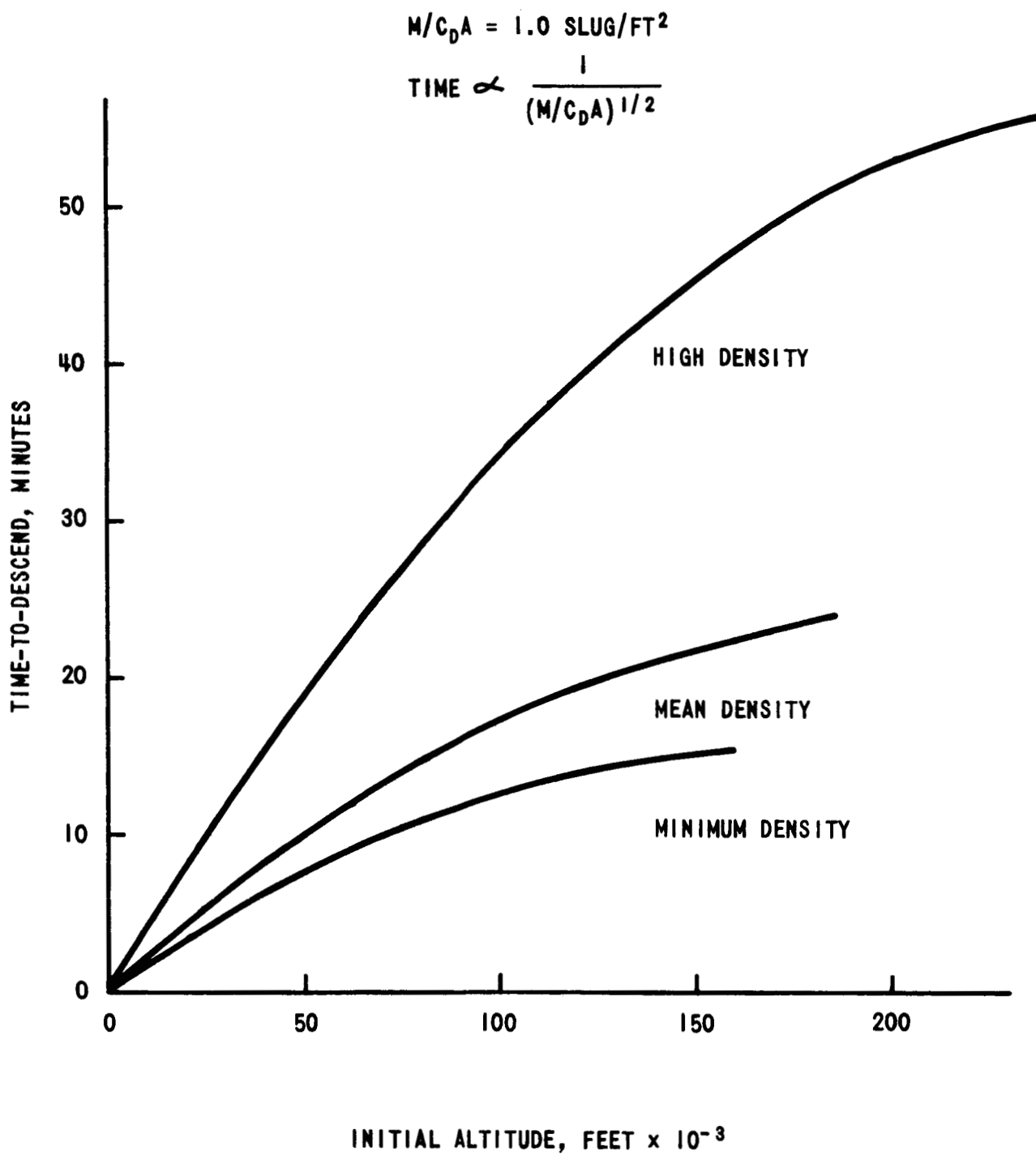


FIGURE 15 TIME-TO-DESCEND FROM ALTITUDE THROUGH VENUS ATMOSPHERE TO S.L.

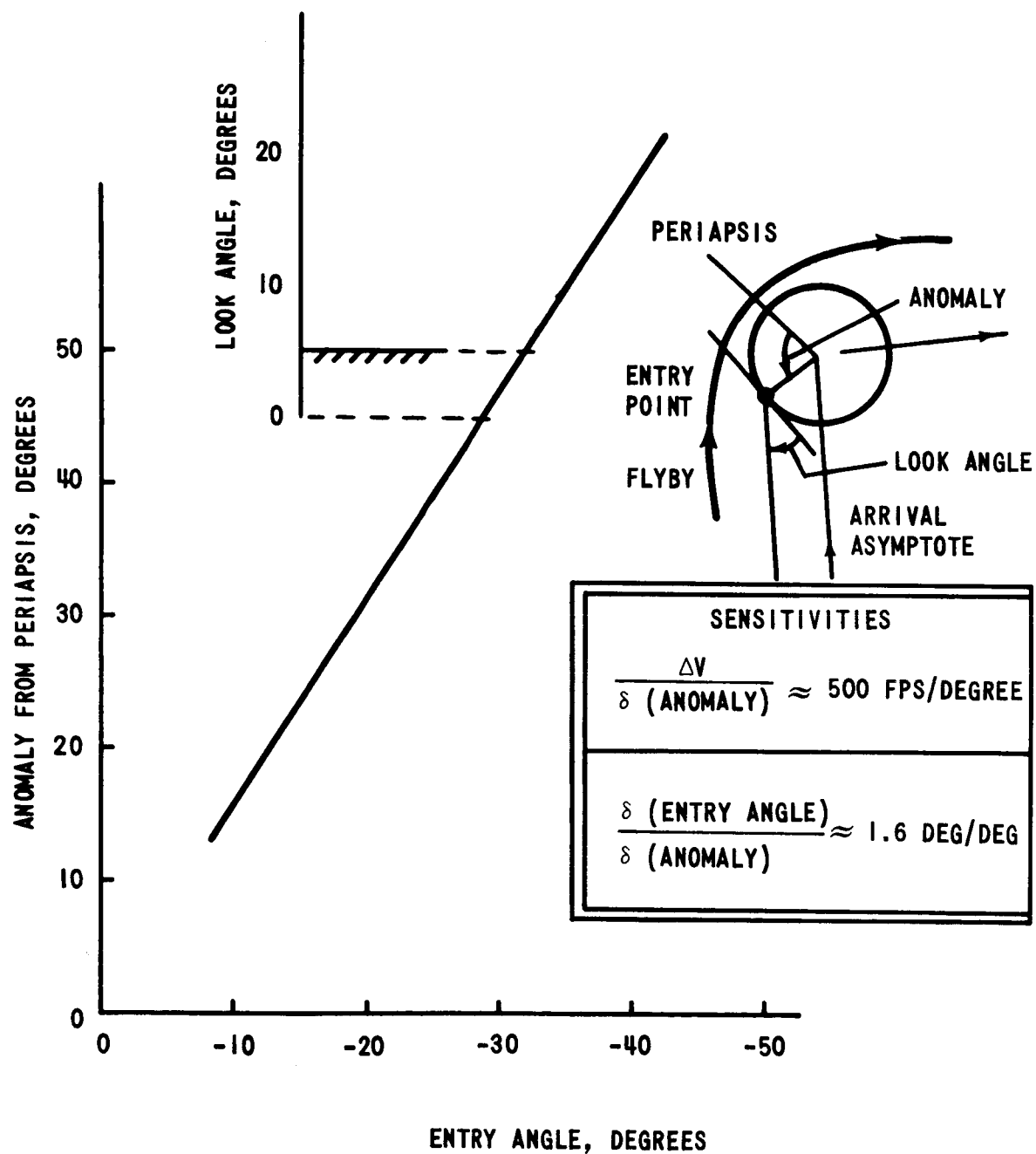


FIGURE 16 ANOMALY ANGLE FROM PERIAPSIS vs. ENTRY FLIGHT PATH ANGLE, 1975 VENUS TWILIGHT FLYBY

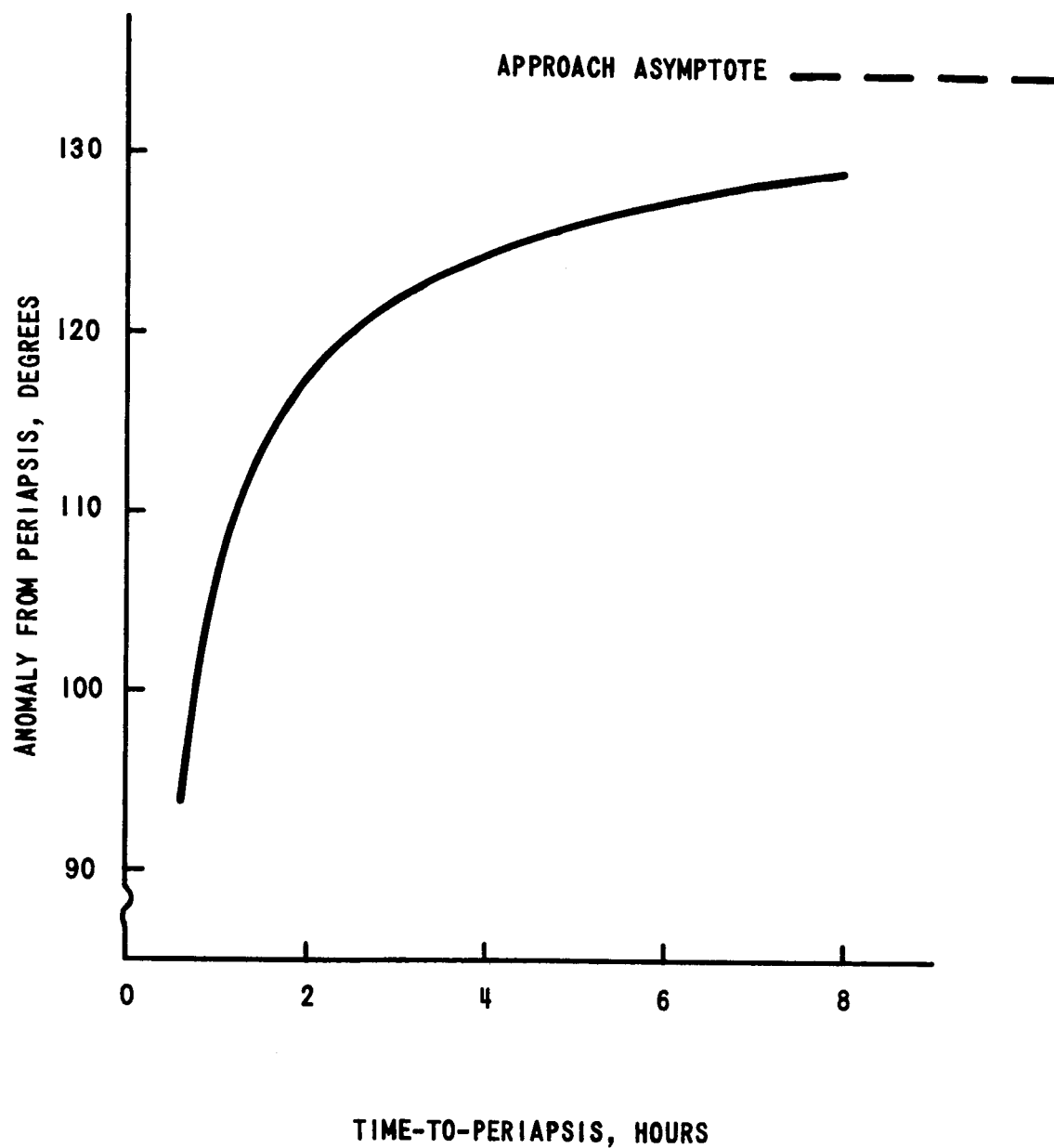


FIGURE 17 ANOMALY ANGLE FROM PERIAPSIS vs. TIME-TO-PERIAPSIS,
1975 VENUS TWILIGHT FLYBY

TABLE I

| ENCOUNTER | TARGET | SUBSOLAR | ANTISOLAR | N. POLE | S. POLE |
|-----------------------------|-----------------|--|---|--|---|
| | | | | | |
| 1975 SINGLE PLANET FLYBY | APPROACH | <u>ANOMALY</u> 41° <u>ENTRY ANGLE</u> -26° <u>VISIBILITY</u> 4° | 41° -26° 4° | 46° -30° 2° | 46° -30° 2° |
| | DEPART | <u>VISIBILITY</u> INVISIBLE | 85° | 0° | 0° |
| 1977 TRIPLE PLANET FLYBY | APPROACH (1) | <u>B*</u> <u>ANOMALY</u> 26° <u>ENTRY ANGLE</u> -16° <u>VISIBILITY</u> -6° | <u>A</u> 38° -24° 6° | <u>B?</u> 88° NEAR VERTICAL 66° | <u>B?</u> 26° BEYOND PERIAPSIS OVERSHOOT INVISIBLE |
| | DEPART (1) | -16° | 16° | 5° | -5° |
| | APPROACH (2) | <u>A</u> <u>ANOMALY</u> 55° <u>ENTRY ANGLE</u> -35° <u>VISIBILITY</u> 26° | <u>B</u> 18° -12° -26° | <u>B</u> 24° -15° -7° | <u>A</u> 36° -23° 7° |
| | DEPART (2) | -2° | 2° | 65° | INVISIBLE |
| 1978 DUAL PLANET FLYBY | APPROACH | <u>A</u> <u>ANOMALY</u> 45° <u>ENTRY ANGLE</u> -28° <u>VISIBILITY</u> 32° | <u>B</u> 7° BEYOND PERIAPSIS OVERSHOOT INVISIBLE | <u>B</u> 23° -14° 6° | <u>B?</u> 13° OVERSHOOT INVISIBLE (6°) |
| | DEPART | INVISIBLE | 60° | INVISIBLE -8° | 8° |

*A - ACCESSIBLE WITH ATMOSPHERIC PROBE

*B - ACCESSIBLE WITH LARGE PROBE